Solidification Crack Susceptibility in Weld Metals of Fully Austenitic Stainless Steels (Report I) †

—Fundamental Investigation on Solidification Behavior of Fully Austenitic and Duplex Microstructures and Effect of Ferrite on Microsegregation—

Yoshiaki ARATA*, Fukuhisa MATSUDA* and Seiji KATAYAMA**

Abstract

It has been well known that weld metals of fully austenitic stainless steels exhibit greater susceptibility to hot cracking and austenitic weld metals containing a small amount (in the order of 5%) of delta (δ) ferrite are much more resistant during welding. However, it has not been clarified completely why the presence of some δ-ferrite prevents hot cracking in Cr-Ni weld metals. Therefore, the authors have investigated the structual change during solidification from a metallographic standpoint for the both weld metals of fully austenitic stainless steel AISI 310S (25Cr-20Ni; Japanese Industrial Standard: SUS 310S) and austenitic stainless steel AISI 304 (18Cr-8Ni; JIS: SUS 304) containing a small amount of δ-ferrite to which sulphur and phosphorus were added as harmful impurities. Each specimen was rapidly quenched in water during TIG arc bead-on-plate welding, so that each bead showed the instantaneous structures from solidification front to room temperature along welding direction. Solidification behaviors of the fully austenitic and the duplex microstructures, microsegregation (especially S and P) during solidification and distribution of alloying elements between δ-and γ-phases at high temperature were investigated.

1. Introduction

Since austenitic stainless steels have good mechanical properties in elevated and low temperature services in addition to an excellent corrosion resistance,they are widely used as various equipment materials of chemical plants, power stations and reactors[1),2)]. Austenitic stainless steels are generally regarded as readily weldable materials, however, the weld metals of fully austenitic stainless steels are susceptible to hot cracking (solidification and ductility-dip cracking). The susceptibility to hot cracking can generally be avoided by using manual or consumable electrodes which contain a small amount of δ-ferrite in weld deposits. However, the ferrite may promote rapid transformation to the brittle sigma phase in service at elevated temperature and lead to preferential attack in certain corrosive environments[3),4)]. Moreover, recently electron beam welding process has been investigated to employ as a welding process of thick stainless steel plates. In such a welding process solidification cracking is a great important problem in welding fully austenitic stainless steels because electrodes are not usually used. Therefore the fully austenitic weld metals which are resistant to solidification cracking are strongly required hereafter[5)6)].

Concerning why the presence of δ-ferrite helps to prevent hot cracking, there are several explanations so far[7)~12)], that is;

(1) Ferrite has a greater solubility than austenite for certain harmful elements and impurities as S, P, Si, etc. The segregation of these elements at the grain boundary and the amount of liquid films can thereby decrease during solidification, and then the boundary does not crack.
(2) The total amount of grain boundaries enlarges.
(3) In a two-phase alloy containing ferrite the γ-grain size would be refined.
(4) The compositions forming some ferrite have a smaller

† Received on Sep. 24, 1976
* Professor
** Graduate Student, Osaka University

solidification range than fully austenitic compositions.
(5) The shrinkage stress is reduced because of a smaller coefficient of thermal expansion of the b.c.c. ferrite.
(6) Liquid films are dispersed by the existence of ferrite, and ferrite strengthens the grain boundary or prevents the formation or propagation of cracks
(7) Ferrite suppresses polygonization process.

Most of explanations on the effect of δ-ferrite are given by the category (1). However, for the authors these were not satisfactorily explained from the metallurgical point of view. The present work, therefore, was undertaken to examine whether the phenomenon explained in (1) actually takes place during solidification. It is generally regarded that the austenitic stainless steel weld metal of AISI 304 (JIS: SUS 304) containing a small amount of δ-ferrite is more resistant to hot cracking than the fully austenitic stainless steel weld metal of AISI 310S (JIS: SUS 310S)[13], therefore commercial SUS 304 and 310S and these modified steels to which S and P were deliberately added were used in this investigation, as S and P are regarded as the most detrimental imprities to promote cracking[7),14)~18)].

Each of these specimens of about 20mm in thickness on which TIG arc bead-on-plate welding was being done without any filler electrodes was rapidly quenched in water to reveal the instantaneous structures during solidification[19)]. Then using these weld metals, the comparisons of the structural change during solidification and the segregation between primary δ-and γ-phases were investigated and particular attention was paid to the effect of the elements S and P on microsegregation in order to investigate the effect of δ-ferrite on segregation and solidification behavior.

2. Experimental Procedure

2-1 Materials used

Chemical compositions of materials used are shown in Table 1. SUS 304 (18%Cr-8%Ni) and SUS 310S (25%Cr-20%Ni) were chosen as representative of austenitic alloys containing δ-ferrite and as a typical fully austenitic composition, respectively. Moreover sulphur and phosphorus elements which promote the susceptibility to hot cracking in general were deliberately increased to commercial SUS 304 and 310S steels so that their effects could be better observed in the investigation of the microstructure and microsegregation. These materials are designated as 304S, 304P, 310S and 310P in Table 1. The specimens welded were disk plates of about 20mm in thickness and about 110 mm in diameter taken from all material ingots.

2-2 Experimental Procedure

Hot cracks of solidification and ductility-dip cracks in weld metals are considered to occur near the solidus temperature and the recrystallization temperature respectively[20)~23)]. Solidification behavior which is important in understanding hot cracking was investigated by quenching each specimen in water during TIG arc bead-on-plate welding without filler metal. TIG arc (DCSP) welding conditions are shown in Table 2. The δ-ferrite content remaining at room temperature, and sulphide and phosphide contents in weld metals during solidification were measured by a point counting method (magnification; x400 or x1000, number of field of vision; 30-100). Electron microprobe analyser (EPMA) and scanning

Table 1 Chemical composition of materials used

Materials (SUS)	Composition (wt%)							
	C	Si	Mn	P	S	Cr	Ni	N
304	0.05	0.63	1.00	0.027	0.004	18.60	9.10	0.0259
304 S-1	0.06	0.60	0.98	0.026	0.023	18.40	9.05	0.0271
304 S-2	0.06	0.60	1.00	0.024	0.081	18.80	9.15	0.0285
304 S-3	0.05	0.56	0.94	0.025	0.220	18.50	9.10	0.0302
304 P-1	0.05	0.58	0.94	0.056	0.006	18.50	9.10	0.0264
304 P-2	0.06	0.61	0.99	0.121	0.005	18.60	9.10	0.0206
304 P-3	0.06	0.60	1.00	0.249	0.005	18.55	9.05	0.0255
310 S	0.07	0.78	1.08	0.022	0.004	24.40	19.90	0.0361
310 S-1	0.07	0.73	1.05	0.022	0.017	24.45	19.90	0.0335
310 S-2	0.07	0.75	1.03	0.023	0.062	24.40	20.00	0.0323
310 S-3	0.06	0.73	1.01	0.023	0.199	24.40	19.95	0.0329
310 P-1	0.06	0.77	1.04	0.055	0.005	23.75	19.55	0.0330
310 P-2	0.06	0.79	1.05	0.109	0.003	23.90	19.80	0.0329
310 P-3	0.06	0.78	1.02	0.240	0.003	24.10	19.67	0.0332

Table 2 TIG arc welding conditions

Welding condition	(1) Low speed	(2) Middle speed	(3) High speed	(4) High speed
Arc voltage (v)	20	17	17	10
Welding current (A)	350	250	250	100
Welding speed (mm/min)	7-25	100	500	600
ThO_2-W electrode (mm)	4	4	3.2	3.2

TIG arc, DCSP, Ar shielding atmosphere

electron microscope (SEM) with the energy-dispersive x-ray spectrometer were used to examine the microsegregation of the elements.

3. Results and Discussion

3-1 Morphology of Solidification Structure

3-1-1 Comparison of Solidification Structure between Commercial SUS 304 and 310S

SUS 304 and 310S plates (20 mmt, 110 mm) taken from ingots were welded under the condition of high weld heat input (E=20(V), I=350(A) and v=20 (mm/min)) to examine the microstructure and the microsegregation by EPMA. Photo. 1 gives an example of a weld bead of SUS 310S obtained by quenching during welding under the above condition. It indicates that a molten pool is almost completely excluded and it gives positions of microstructures shown in Photos. 2 and 3 which show the typical structures near solidification front of SUS 304 and 310S weld metals respectively. The upper part of Photos.2(a), 2(b), 3(a) and 3(b) shown in low magnification (x100) indicates that this area was completely liquid in the molten pool at the moment of quenching, and the lower part shows the region of lower temperature. Photos. 2(c) to 2(h) and 3(c) to 3(f) show the instantaneous microstructures quenched rapidly from temperatures from solidification front to room temperature or to about 1150°C in higher manification (x400).

In case of SUS 304 weld metal etched in Kalling's reagent or aqua regia (nitric-hydrochloric acid) reagent, δ-ferrite appears dark or black and γ-phase has a brighter or white appearance. It can be known from the dark impression of Photo. 2(a) and (b) that the structure from SUS 304 weld metal is roughly characteristic of the mode of cellular dendritic growth. Photo.2(c) shows the structure of the tips of dendrite stems close to the solidification front and indicates that cellular dendrite stems were formed as δ-ferrite in the initial stages of solidification. Furthermore, in quenching the primary δ-ferrite was transformed to Widmanstätten phase by rapid cooling and the remaining liquid was solidified as

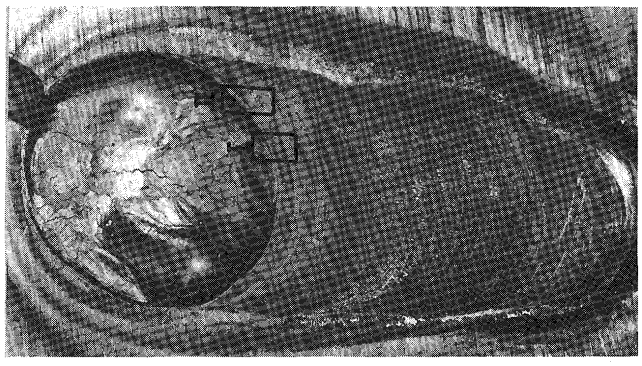

Photo. 1 Surface appearance of SUS 310S weld bead quenched in water during welding at high weld heat input of 350A, 20V and 20 mm/min, and I and II give positions of (a) and (b) in Photos. 2 and 3.

the eutectic δ- and γ-phases or chiefly as γ-phase. The microstructure close to the last stages of solidification is shown in Photo. 2(d). It indicates that a large amount of primary δ-ferrite was formed in the dendrite stems and subsequently the eutectic δ-and γ-phases began to be formed in the interdendritic liquid. However, the ferrite was transformed to Widmanstätten austenite during quenching. Photo.2(e) probably shows the region where the ferrite was a little transformed to the austenite near the cellular dendritic boundary soon after the completion of the solidification, and indicates that part of the dendrite arms of the ferrite connected hand in hand due to the presence of the primary and the eutectic ferrite and dendrite stems of the ferrite were transformed to Widmanstätten austenite during quenching. The microstructure in Photo. 2(f) at a little lower temprature during cooling than Photo. 2(d) indicates that the ferrite was transformed further to the austenite. Photo. 2(g) shows the region at a distance of about 5 mm behind the solidification front and the temperature is about 1200°C from the result measured with a calibrated W·5%Re-W·26%Re thermocouples immersed in the weld pool. It reveals that most of the ferrite was transformed to the austenite. Photo.2(h) shows the structure at room temperature. The ferrite remained in an interlocked or

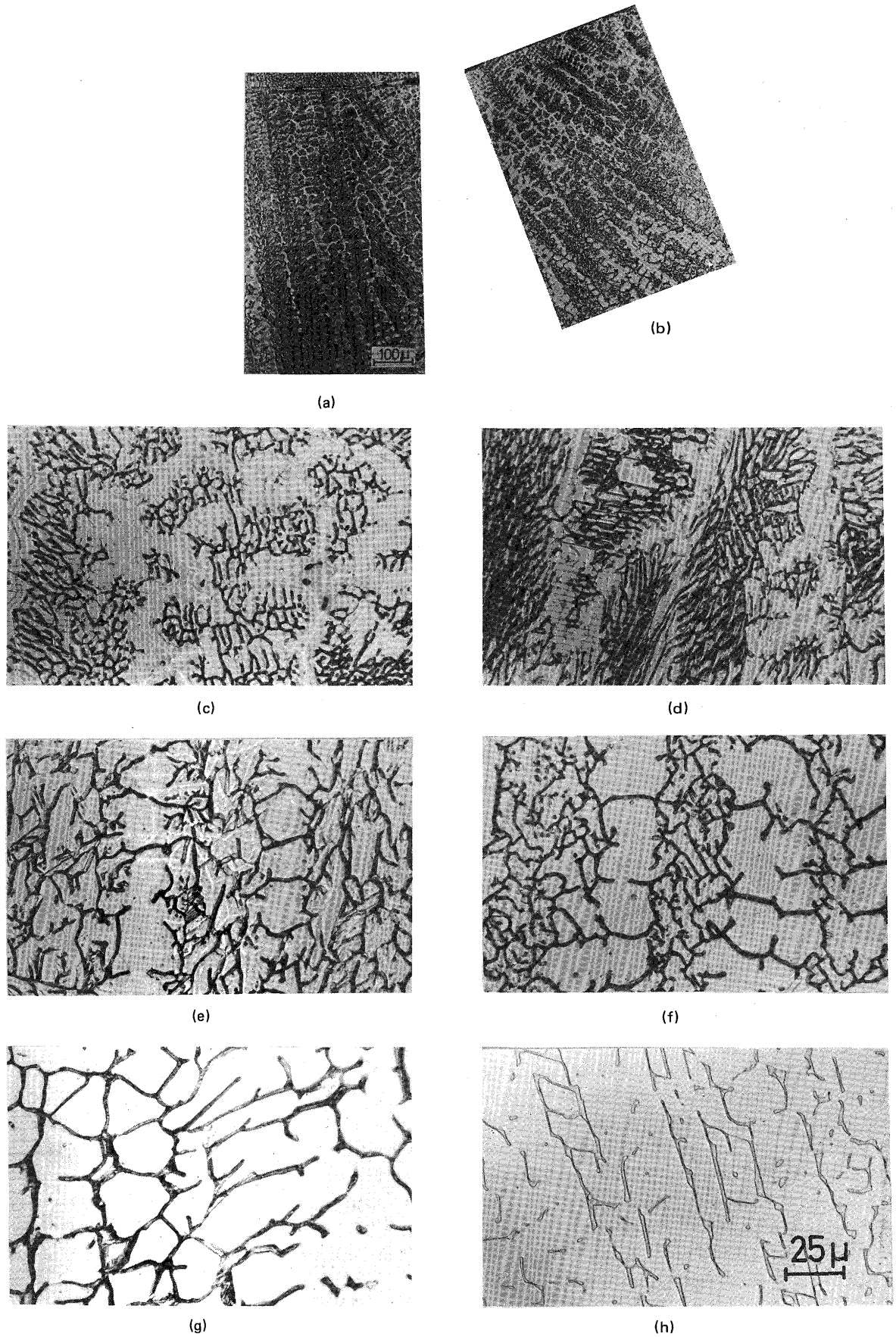

(a) (b) (c) (d) (e) (f) (g) (h)

Photo. 2 Microstructures from solidification interface to room temperature of SUS 304 weld metal. (a), (b) in low magnification (x100); (c) to (h) in high magnification (x400).

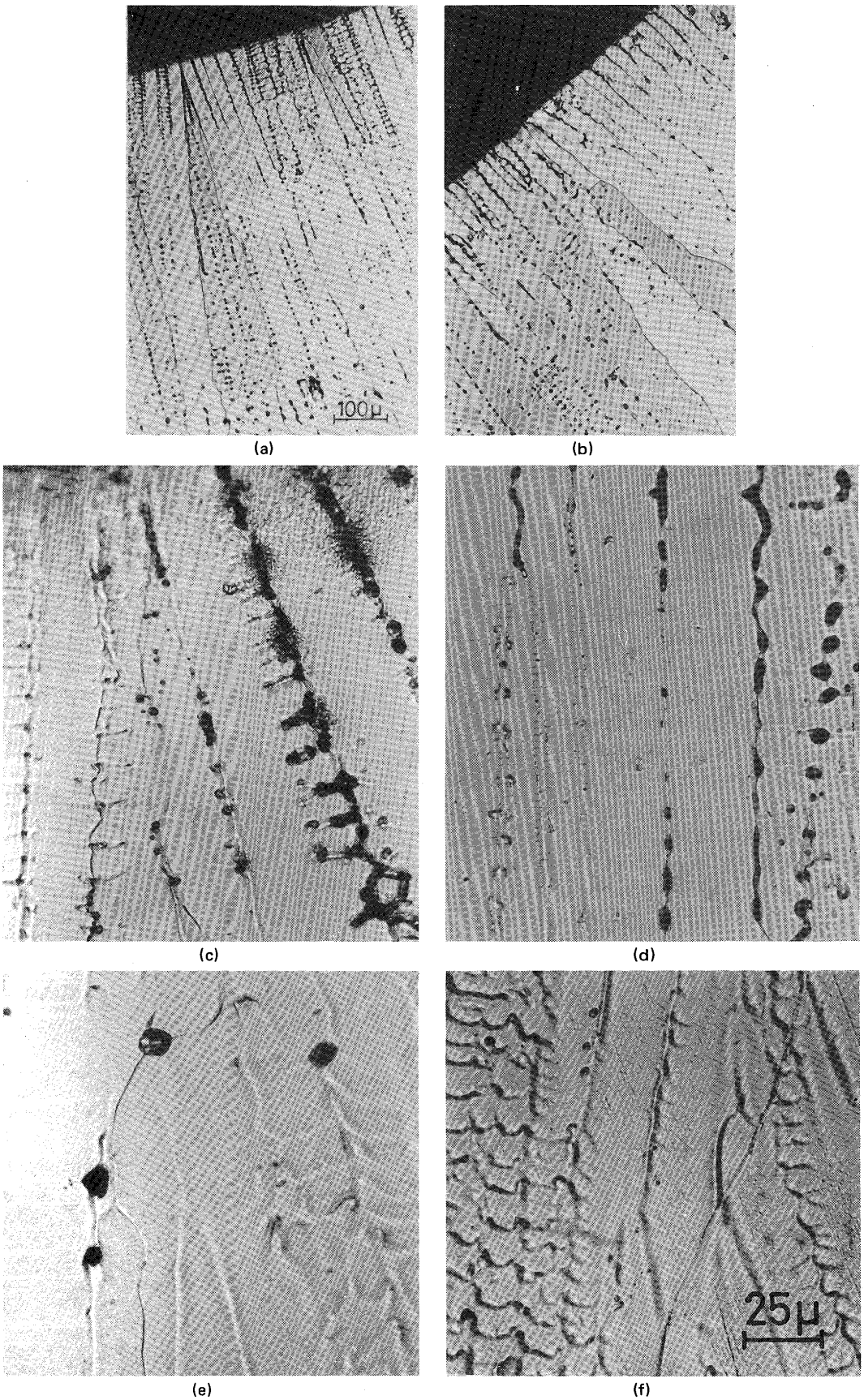

Photo. 3 Microstructures near solidification interface of SUS 310S weld metal. (a), (b) in low magnification (x100); (c) to (f) in high magnification (x400).

island-like form. This structure is quite ordinarily seen in the weld metals containing the ferrite. As a result of the above observation the microstructures suggest the solidification process of SUS 304 in the following way. During the initial stages of solidification the advancing cellular dendrites grow in the liquid and form as δ-ferrite. In the last stages of the solidification the eutectic δ-and γ-phases are formed in the cellular dendritic boundary. As soon as solidification completes the γ-phase grows into the primary δ-ferrite as a result of the transformation of ferrite to austenite. Moreover, during subsequent cooling the primary and the eutectic ferrite is largely transformed to the austenite, which results in a small content of the residual δ-ferrite measured at room temperature.

The structure from SUS 310S weld metal etched in aqua regia reagent is also cellular dendritic mode as shown in Photo. 3(a) and (b).The structure near the solidification front is shown in Photo. 3(c). It indicates that the tips of dindrite stems of the austenite were advancing in the liquid and still a large proportion of liquid was remaining in the cellular dendritic boundary and was solidified during quenching. Photo. 3(d) also shows that film-like liquid was remaining in the cellular dendritic boundary. Photo. 3(e) shows the region at about 1 mm behind the solidification front where small lakes of liquid were enclosed in the solid. Photo. 3(f) shows the region at about 1150°C at about 7 mm behind the solidification front where the migraged boundary is observed. As above results the solidification process of SUS 310S weld metal is suggested as follows. The austenite is formed as a cellular dendritic mode from the initial to the last stages of solidification, and in the last stages film-like liquid and small lakes of liquid appear to be formed along cellular dendritic and grain boundaries. During the subsequent cooling the grain boundaries begin to migrate in the solid. The ferrite does not appear at any temperature during welding.

Concentration distribution of Cr and Ni elements in the dendritic cells in the final stages of the solidification at the moment of quenching was transversely analyzed by EPMA (the beam diameter: about 2 to 5μ). It is shown in Fig. 1 (a) and (b) which correspond to SUS 304 and 310S weld metals respectively. In case of SUS 304 the composition of cellular dendrite stem consists of 19.5% Cr and 7.2%Ni, and consequently that of the boundary shows a low level of Cr and a high level of Ni. In case of SUS 310S the composition of cellular dendrite stem consists of 23.4%Cr and 19.3%Ni and that of the boundary shows 27%Cr and 20.4%Ni. The segregation ratio (C_{Max}/C_{Min}) of Cr is about 1.15 and that of Ni is 1.06 in the primary austenite of SUS 310S. Moreover, the concentration at the center of dendrite stem and the grain boundary is drawn in Fig. 2 which shows the solidus surface of the Cr-Ni-Fe system[26]. It will give evidence as follows as well as the above explanation. In case of SUS 304 dendrite stems were solidified as the primary phase of the ferrite which has low Ni content, and the austenite was formed in the final stages of solidification. Moreover, in case of SUS 310S the primary phase of austenite was formed

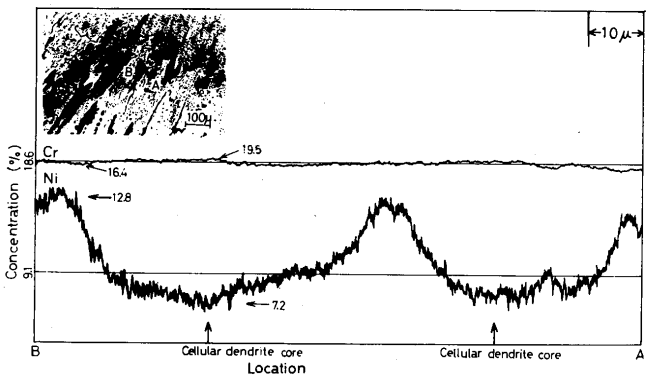

(a)

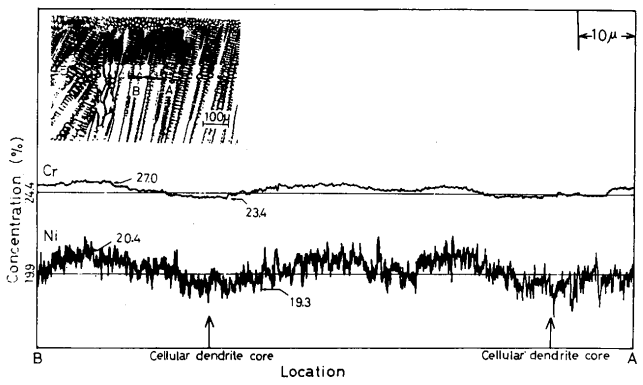

(b)

Fig. 1 Concentration distribution of Cr and Ni in cellular dendrite in final stages of solidification of SUS 304 (a) and 310S (b) weld metals.

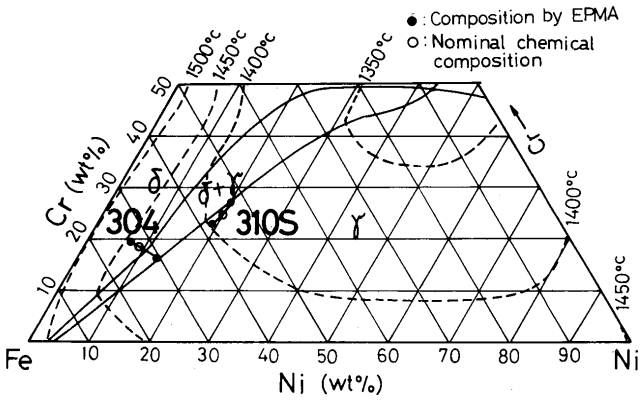

Fig. 2 Solidus surface of Fe-Ni-Cr system[26] and distribution of elements during solidification in 304 and 310S weld metals.

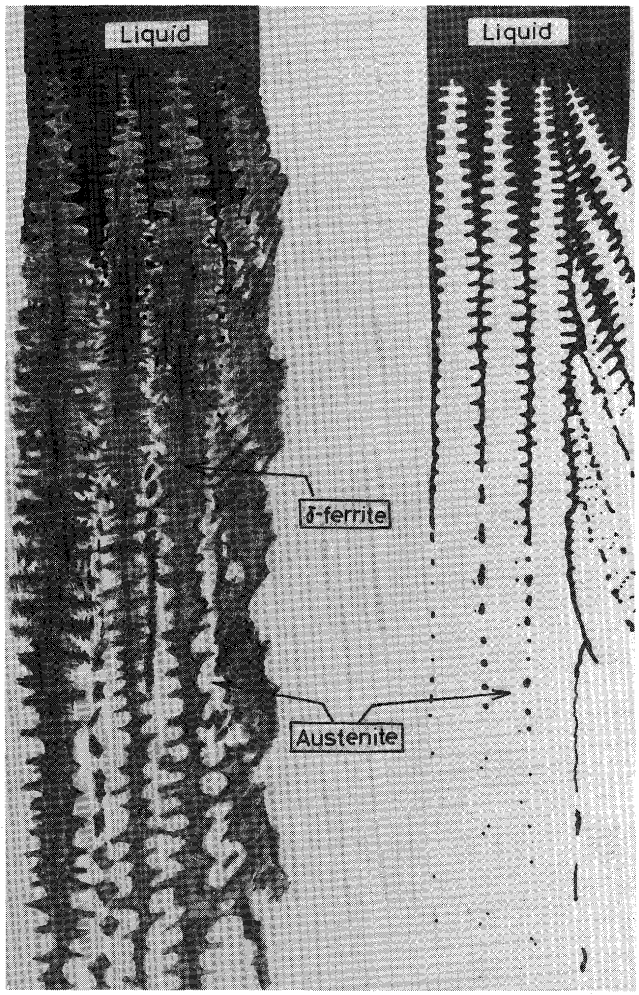

Fig. 3 Schematic representation of solid-liquid interface of austenitic stainless steels during solidification in 304 and 310S weld metals.

from the initial to the last stages of solidification and the ferrite was not formed. From the above photos and results the schematic representation is considered in Fig. 3 on the morphology of the solidification structures during welding of SUS 304 and 310S.

3-1-2 Change of δ-Ferrite

It is very difficult to understand the solidification structure from the structure of the weld of austenitic stainless steel containing δ-ferrite because of complicated morphology of δ-ferrite at room temperature. Therefore it seems valuable to observe the change of the ferrite phase dependent on temperature from the final stages of solidification to room temperature. An example is shown in Photo. 4, which was welded under the welding condition of I = 350A, E = 20V and v = 7mm/min. It will be enough to have explained in the 3-1-1 concerning the solidification process. During solidification the primary δ-ferrite occurred to a degree of about 80% in area. However, during cooling after solifification the content of δ-ferrite decreased drastically at high temperature of around 1300°C and later did not vary largely. At room temperature the ferrite remains in a lacy, interlocked dendritic or fine needle-to-disk form. The morphology of the ferrite, i.e., its shape, size and distribution is affected by weld heat input. Photo. 5 shows the structures of weld heat input from 1 to 600 (KJ/cm). The ferrite is becoming finer with an increase in a freezing rate at low weld heat input. The result of SUS 304 weld metal indicates that the redisual δ-ferrite content at room temperature was not largely varied within 1% in difference in area to area at constant weld heat input. Moreover, the relationship between the weld heat input and the residual δ-ferrite content was investigated for SUS 304 weld metal in Fig. 4. As the weld heat input increased from 1 to 600 KJ/cm, the residual ferrite content showed a tendency to increase from about 3.6 to about 6%.Furthermore, the primary ferrite content also showed a similar tendency to increase from 75 to 80%. Therefore, from this result we should actually pay attention to such a large amount of the primary δ-ferrite during solidification which disappears during cooling, in case of austenitic stainless steel weld metal containing δ-ferrite. We should also pay attention that the large amount of the primary δ-ferrite affects strongly the

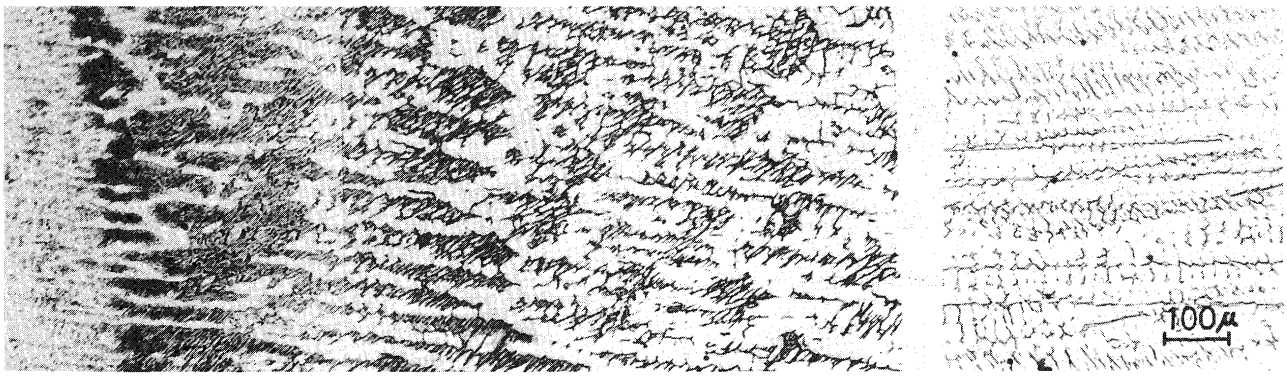

Photo. 4 Change of δ-ferrite phase dependent on temperature from (left) final stages of solidication to (right) room temperature in SUS 304 weld metal.

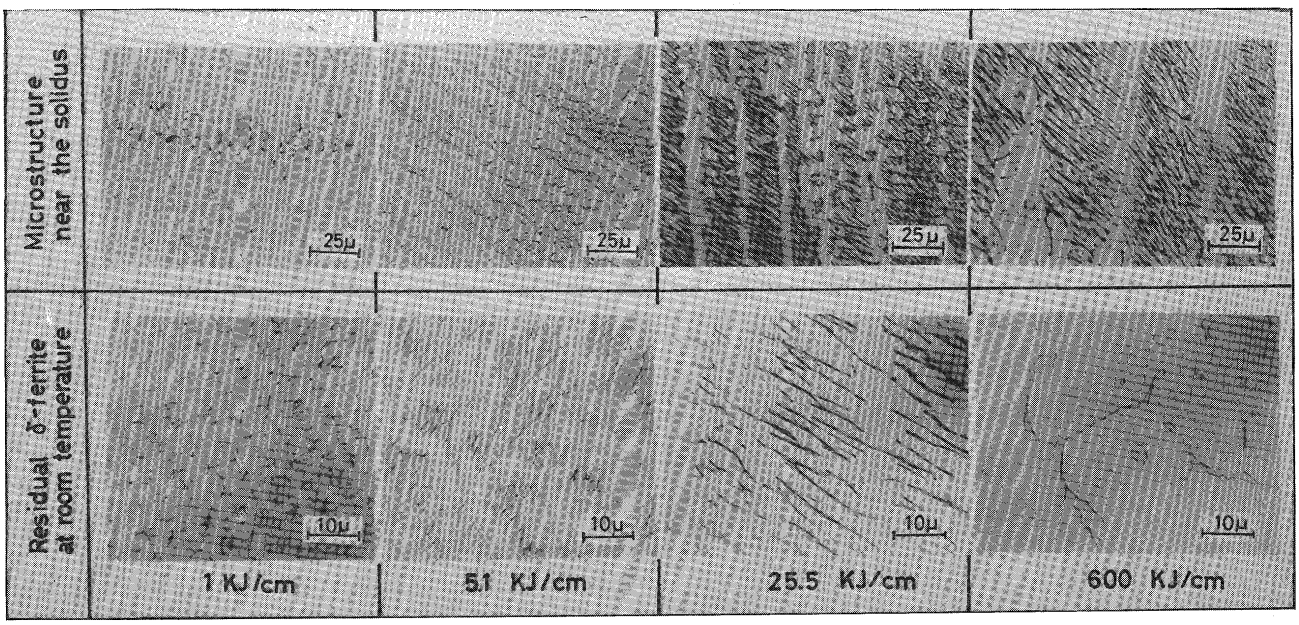

Photo. 5 Comparison of microstructures near the solidus (upper) and at room temperature (lower) dependent on variation of weld heat input.

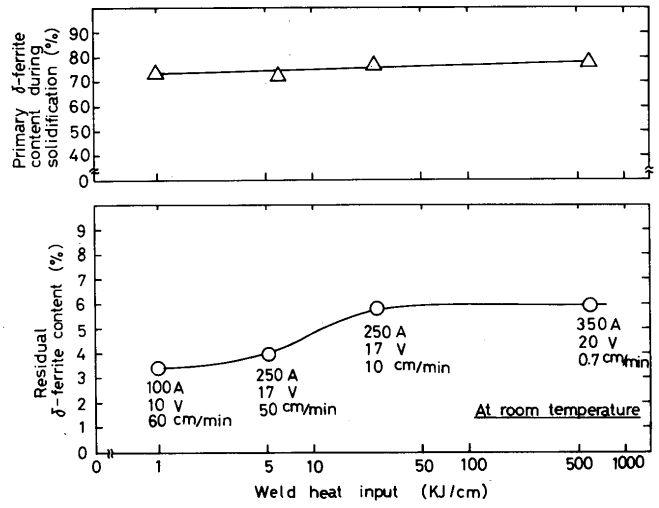

Fig. 4 Effect of weld heat input on primary ferrite content in area during solidification and residual ferrite content at room temperature.

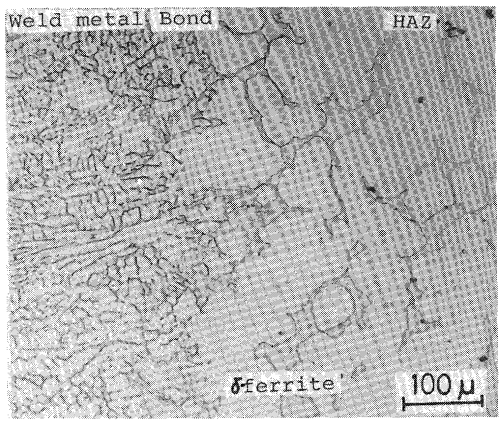

Photo. 6 Microstructure of SUS 304 weld shows large δ-ferrite in HAZ quenched form high temperature.

susceptibility to hot cracking. Therefore the effect of the amount of the ferrite at room temperature on hot cracking susceptibility of austenitic stainless steel weld metal should be primarily investigated by replacing with the amount of the primary δ-ferrite during solidification.

3-2 Microsegregation during Solidification

3-2-1 Equilibrium Distribution of Alloying Elements between δ-and γ-phases.

Photo. 6 shows the structure near fusion boundary of SUS 304 welded at the high weld heat input. Since this area (within 1 mm from bond) was maintained at high temperature near the melting point for a relatively long time, δ-ferrite grew large enough. Therefore the equilibrium distribution of alloying elements at high temperature is expected between δ-and γ-phases. Thus this kind of large ferrite and the austenitic matrix were analyzed by EPMA to investigate their distribution. The results are summarized in Fig. 5. The compositions of Fe, Cr, Ni, Mn, Si elements are given at calculated value (wt%) according to EPMA diagram to correct and C, S and P elements are shown at the number of count per second. Fe, Ni, Mn, and C were more soluble in the γ-phase, and Cr, S and P were more soluble in the ferrite. Si was not detected in a definite difference in this investigation. These results indi-

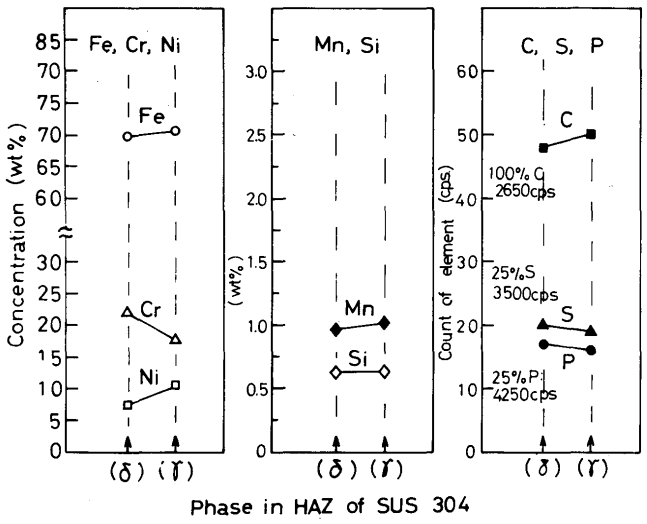

Fig. 5 EPMA analyses of Fe, Cr, Ni, Mn, Si, C, S and P between δ-and γ-phases in HAZ of SUS weld quenched form high temperature.

cate that austenitizers (austenite-forming elements) in iron such as Ni, Mn and C are more soluble in the γ-phase and ferritizers (ferrite-forming elements) such as Cr are more soluble in the ferrite. Moreover, a little larger quantities of S and P were contained in the ferrite. That is probably because the ferrite has a large capacity for dissorving S and P according to the equilibrium diagram[7]. The above-mentioned results show the same tendency as the general explanations since the earlier literature[7),27)].

3-2-2 Microsegregation during Solidification

Distribution or segregation of each element is one of the most important factors relative to hot cracking. Therefore, EPMA line analyses were carried out transversely to dendrite stems in the final stages of solidification of SUS 304 and 310S weld metals of the high weld heat input. Fig. 6(a) and (b) show examples of the distibution of each element in the final stages of solidification for SUS 304 and 310S weld metals respectively. The compositions in cellular dendrite core and at the boundary in the final

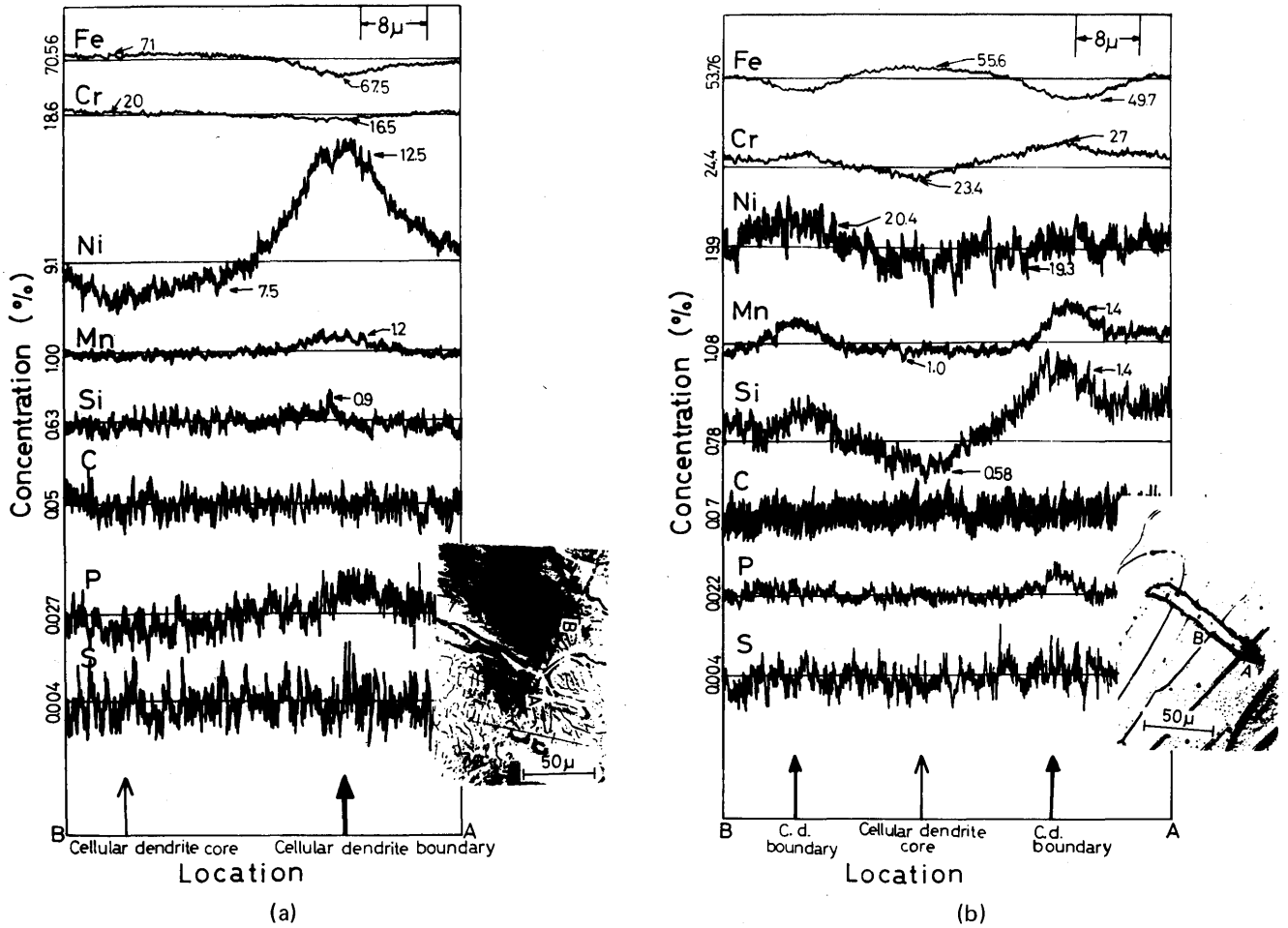

Fig. 6 Concentration distribution of each alloying element in final stages of solidification in SUS 304 (a) and 310S(b) weld metals.

stages of solidification are summarized in Fig. 7 for SUS 304 and 310S weld metals.

In SUS 304 weld metal Fe and Cr were rich and Ni was poor in the cellular dendrite stem of the ferrite. Consequently Ni segregated in the cellular dendritic boundary of the austenite. In SUS 310S weld metal Cr and Ni were poor in cellular dendrite stem and segregated in the boundary. S, P, Si and Mn segregated in the boundaries in both SUS 304 and 310S weld metals. The segregation of C in the boundary could not be detected because C could probably diffuse into the solid during solidification due to the higher diffusivity into the solid. Si, S and P segregated in the boundary even in SUS 304 weld metal. This differs in the tendency for the distribution between δ-and γ-phases in the heat affected zone (HAZ) of SUS 304 weld, mentioned in the 3-2-1. This means that the segregation of each element is determined by its distribution coefficient during solidification. There is an obvious feature between SUS 304 and 310S weld metals that the segregation of P and Si was more noticeable in SUS 310S than SUS 304. This suggests that SUS 310S weld is more susceptible to hot cracking.

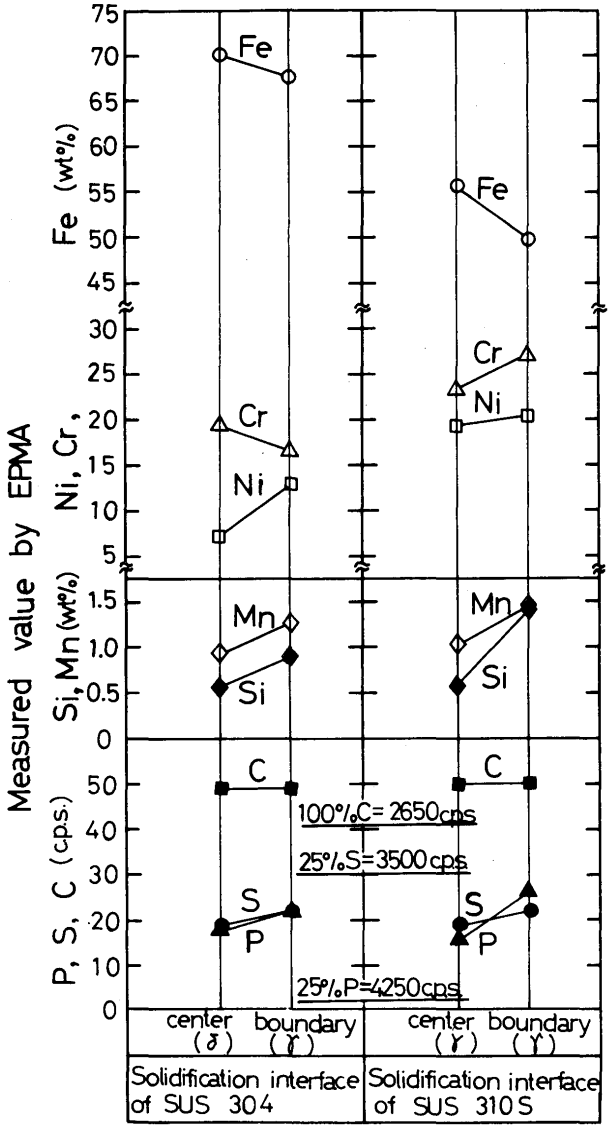

Fig. 7 EPMA analyses of each alloying element in cellular dendrite core and at boundary of SUS 304 (left) and 310S (right) weld metal.

3-2-3 Microconstituents in SUS 304 and 310S Weld Metals

By using the energy-dispersive x-ray spectrometer of the SEM, efforts were made to find out inclusions which may be related to solidification cracking. In case of SUS 304 weld metal, in consequence of the SEM spot analyses two kinds of inclusions were found out as shown in Fig. 8(a) and (b). Some inclusions enriched in P are phosphides as shown in (a) and the other enriched in Al, Mn, Si and others are perhaps oxides as shown in (b). The SEM microstructure near the solidification front of SUS 304 weld metal is shown in high magnification (x2000) in Photo.7. In it δ-ferrite etched deeply is hollow and two inclusions are seen in the matrix of the austenite which would correspond to the cellular dendritic boundary during solidification. A few phosphides were observed only in the region near the solidification front. They were formed predominantly in the boundaries because a large amount of interdendritic liquid close to the front would be solidified due to the quench. More oxides were observed in the granular or grobular form in any areas. In case of SUS 310S weld metal the SEM results of the inclusions detected are shown in Fig. 9, and Fig. 9(a), (b), (c) and (d) indicate evidence of phosphide, sulphide, oxide and silicide respectively, Phosphides are enriched in P and Cr with respect to the matrix, sulphides are enriched in S and Mn and contained Cr and Fe, oxides are enriched in Al, Si, Mn and others, and silicides consist of Si, Fe, Cr and Ni. Moreover, the SEM microstructures near the solidifica-

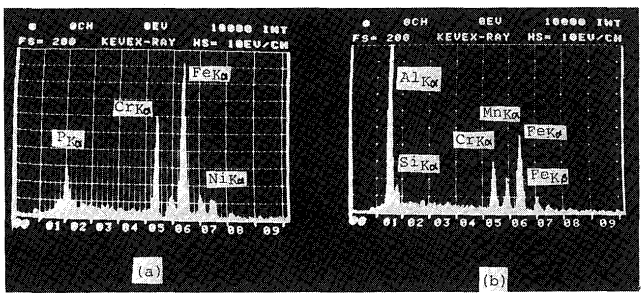

Fig. 8 SEM energy-dispersive x-ray spectrometer results of phosphide (a) and oxide (b) in SUS 304 weld metal.

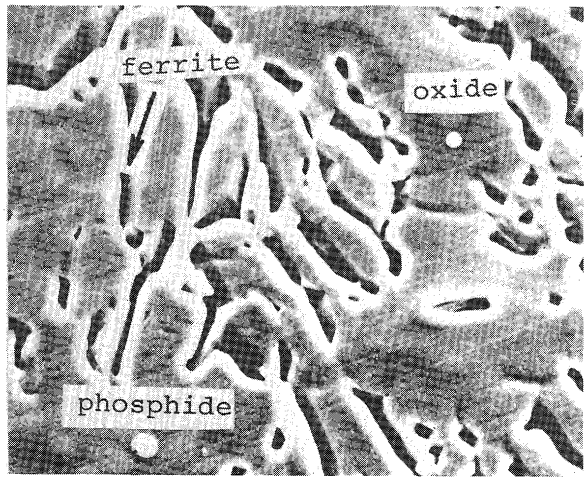

Photo. 7 SEM microstructure near solidification interface of SUS 304 weld metal shows phosphide and oxide.

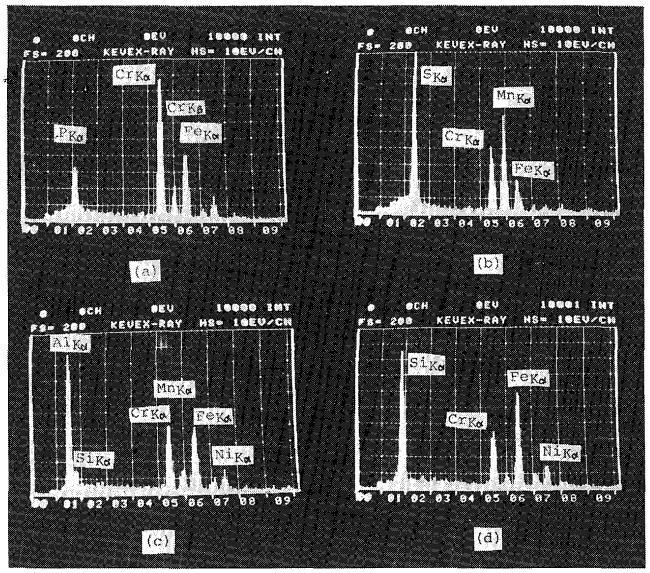

Fig.9 SEM analytical results of phosphide (a), sulphide (b), oxide (c), silicide (d) in SUS 310S weld metal.

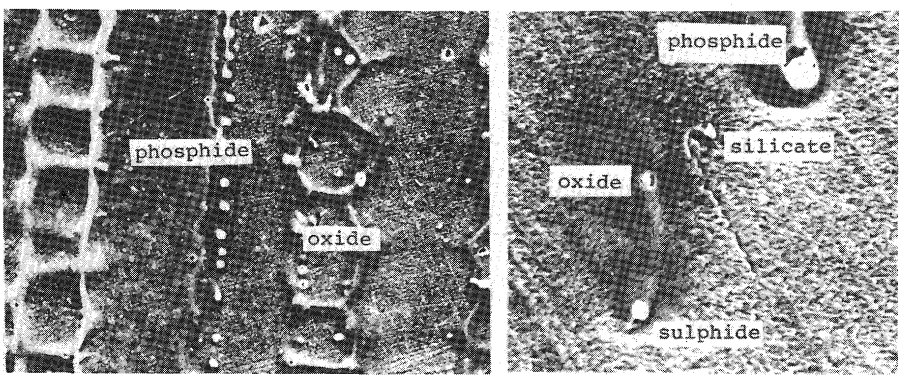

(a) (b)

Photo. 8 SEM microstructures near solidification interface (a) and at low temperature (b) of SUS 310S weld metal show more inclusions at boundary.

tion front and at region below the solidus temperature are shown in Photo. 8(a) and (b). It is clearly shown from Photo. 8(a) near the front that a lot of inclusions were formed in the cellular dendritic boundaries. Most of them were phospides and oxides. These phosphides were enriched in P and Cr and sometimes contained S and Si together because the interdentritic liquid would have solidified by quenching. In regions below the solidus the inclusions such as phosphide, sulphide, oxide and silicate as shown in Photo. 8(b) were observed predominantly in the cellular dendritic and grain boundaries.

3-3 Effect of Sulphur or Phosphorus added on Microsegregation during Solidification

3-3-1 Effect of Sulphur on Microsegregation

Photo. 9 shows the quenched structure near the solidification interface (a) and at about 1100°C during cooling (b) of SUS 304 S-3 weld metal containing 0.22%S welded at the high weld heat input in high magnification to observe sulphides. δ-ferrite in Photo. 9(a) is dark and in a fine needle form due to the Widmansttäten precipitation during quenching and the ferrite in Photo. 9(b) is dendritic mode due to the transformation of the ferrite to the austenite, and the austenite is brighter matrix. The inclusions are in black (actually dark red) granular form and their size is about 0.2 to 2.0μ. They are in fact sulphides from the results analyzed be EPMA and SEM.

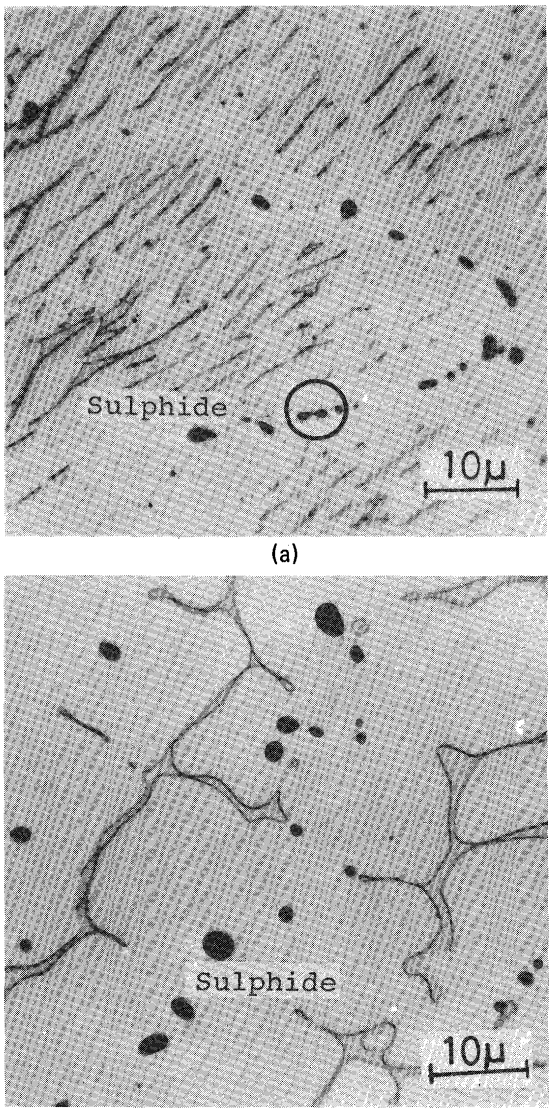

Photo. 9 Microstructures of 304 S-3 weld metal containing 0.22%S near solidification interface (a) and at about 1100°C (b).

The latter result shown in Fig. 10 indicates that sulphides are enriched in S and Mn and depleted in Fe and Ni with respect to the matrix. Sulphides may become in granular or rod-like form due to the effect of Mn. It is observed that almost all sulphides were formed in the cellular dendritic and columnar grain boundaries during solidification as shown in Photo. 9. Moreover, as shown in Photo. 9(b) sulphides in the structures at any temperatures after the completion of solidification were mainly formed in the matrix of the austenite, which seems to correspond to the cellular dendritic boundaries in the last stages of solidification.

The microstructures of SUS 310S-3 weld metal containing about 0.2%S are shown in Photo. 10. The area of Photo. 10(a) and (b) was quenched from the condition in the existence of residual liquid in the boundary Photo. 10(c) shows the structure at about 1200°C. A string of sulphides was formed in the granular or rod-like form in each cellular dendritic boundary. In Photo.10(c) the migrated boundary is pinned by sulphides. The size was from 0.2 to 3.0μ.

The analytical result of SEM of sulphides is shown in Fig. 11. The sulphides were enriched in Mn, Cr and S and depleted in Fe and Ni with respect to the matrix. There-

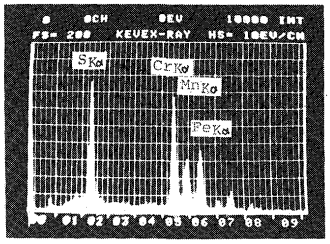

Fig. 10 SEM result of sulphide in 304 S-3 weld metal shows enrichment of S, Cr and Mn.

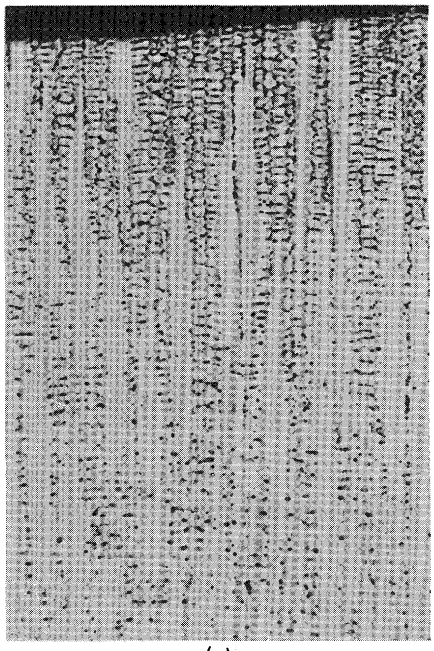
(a)

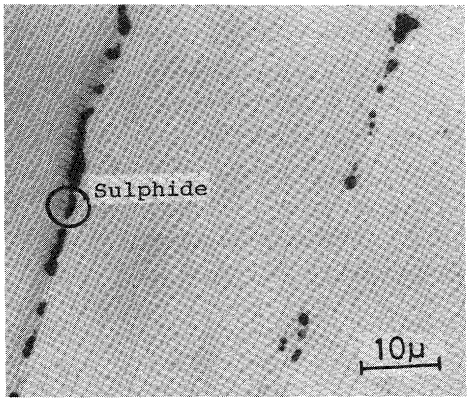

(b)

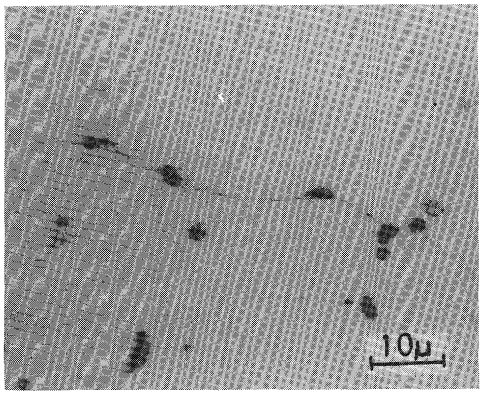

(c)

Photo. 10 Microstructures of 310 S-3 weld metal containing 0.2%S near solidification interface (a), in high magnification (b), and at about 1200° C (c).

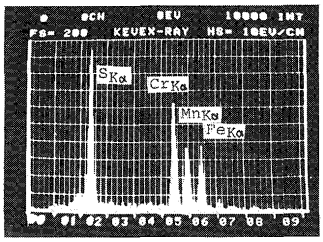

Fig. 11 SEM result of suphide in 310 S-3 weld metal shows enrichment of S, Cr and Mn.

fore they are thought to be M(Mn, Cr, Fe, Ni, etc.) S type and the cracking tendency will be reduced by the fact that S combines chiefly with Mn and consequently the shape of sulphides becomes granular.

In area in the final stages of solidification in SUS 304 and 310S weld metals containing from 0.004 to 0.22%S, the S content in the cellular dendrite core was analyzed by EPMA and subsequently the amount of sulphides predominantly at the cellular dentritic boundary was measured by a point counting method. The results are shown in Fig. 12. It was impossible to detect a clear difference in the S solubility at the dendrite core between SUS 304 (δ-phase) and SUS 310S (γ-phase) even if the S content added is high. However, although the amount of sulphides increases proportionately with an increase in the S content added, there was a relatively large difference in the amount of sulphides between SUS 304 and 310S weld metals. Take 0.05%S for example, the amount of sulphides was 0.05% in SUS 304 weld metal and 0.2% in SUS 310S weld metal. This suggests that S segregates more easily along the cellular dendritic and columnar grain boundaries in SUS 310S weld metal which solidifies primarily as γ-phase than in SUS 304 weld metal which solidifies primarily as δ-phase.

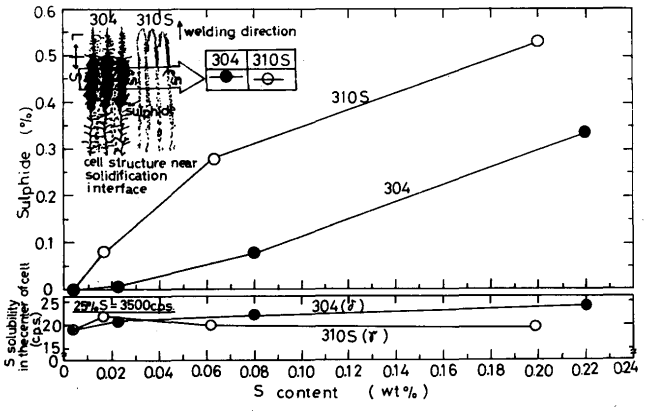

Fig. 12 Comparison of S solubility in cellular dendrite core and consequently sulphide content in weld metals in final stages of solidification between SUS 304 and 310S.

3-3-2 Effect of Phosphorus on Microsegregation

The structures of SUS 304 P-3 weld metal containing about 0.25%P are shown in Photo. 11. The weld metal was quenched during welding under the condition of 350A, 20V and 20mm/min. Photo. 11(a) and (b) show the structures near the solidification interface in low and high magnification, respectively. Photo. 11(c) shows the structure a little away from the interface. The microstructure and the analytical result of the SEM of phosphide are shown in Fig. 13. It was found that the phosphide was enriched in Cr and P and depleted in Ni with respect to the matrix, so that it would consist of the eutectic of (Fe, Cr, Ni)-(Fe, Cr, Ni, etc.) $_3$P. A few phosphides were formed in the granular form in the cellular dendritic boundary of the austenite as shown in Photo. 11(b). These reveal small lakes of liquid which were enclosed in the solid during the solidification process and led to phosphides due to the quench. In the areas as shown in Photo. 11(c) the ferrite was transformed to the austenite and phosphides disappeared. It is supposed that P disssolved in the matrix during cooling slowly after solidification. It was very difficult to find out phosphides through the optical microscope as the weld heat input decreased, even if SUS 304 weld metal contained about 0.25%P.

Concerning SUS 310P-3 weld metal containing about 0.24%P, the structures are shown in Photo. 12. Photo. 12(a) and (b) show the structures near the solidification interface and at about 2.4mm behind the interface, and Photo. 12(c) and (d) show the areas at about 1250°C and 1100°C respectively. The analytical result of the SEM of phosphide is shown in Fig. 14. It indicates that the phosphide is enriched in Cr and P and depleted in Fe and Ni with respect to the matrix. In the areas near the solidifi-

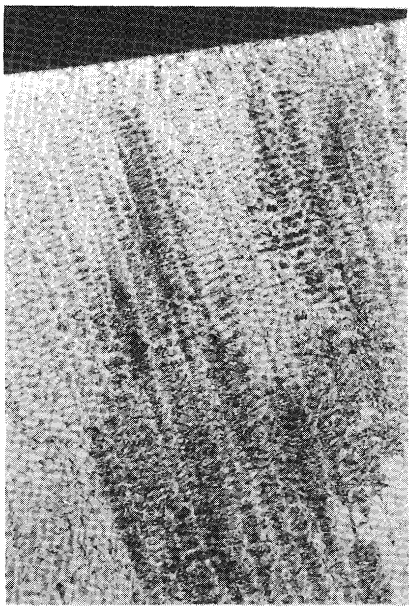

(a)

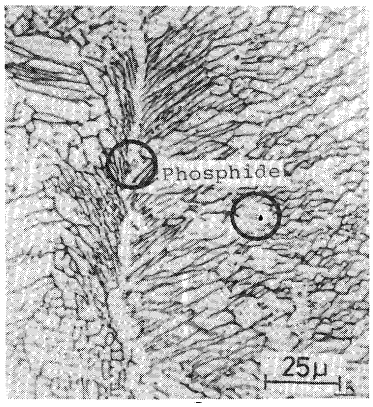

(b)

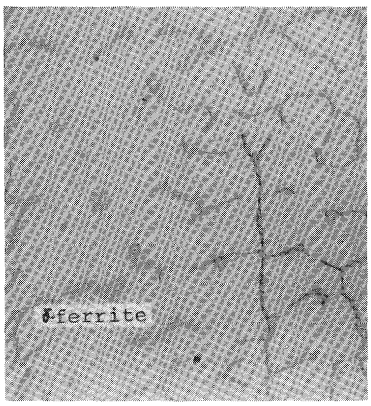

(c)

Photo 11 Microstructures of 304 P-3 weld metal, near solidification interface in low (a) and high (b) magnification and a little away from the interface (c) showing ferrite after transformation.

cation interface a large number of film-like phosphides were formed along both the cellular dendritic and the grain boundaries as shown in Photo. 12(a) and in the

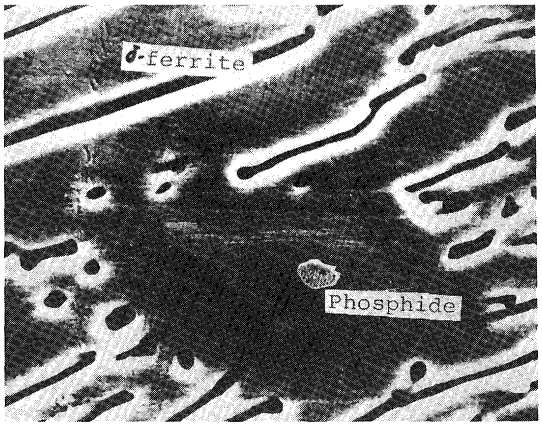

(a)

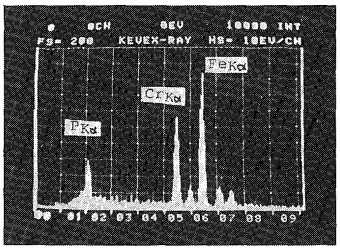

(b)

Fig. 13 SEM result of phosphide in 304 P-3 weld metal shows a phosphide in austenite (a) and enrichment of P, Cr and Fe(b).

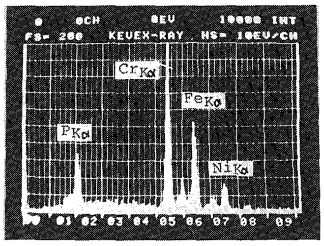

Fig. 14 SEM result of phosphide in 310 P-3 weld metal shows enrichment of P and Cr.

upper of Photo. 12(b). This means that the film-like liquid remained in the boundaries because of a low solidification temperature and was solidified due to the quench. In case of the high weld heat input the phosphides were mainly formed in a rod-like form at the cellular dendritic boundary in a film-like form at the grain boundary as shown in Photo. 12(d). However, in case of the weld metal containing 0.24%P and low weld heat input or rapid cooling rate the phosphides tended to be formed in the film-like form both at the cellular dencritic boundary and at the grain boundary.

Fig. 15 shows the comparison of the P solubility in the cellular dendrite core and consequently the amount of phosphides at the boundaries in the final stages of solidification between SUS 304 and 310S weld metals, which contained from 0.02 to 0.25%P. The P solubility analyzed

by EPMA was shown by the counts per second (c.p.s.) in the lower part and the amount of phosphides measured by the point counting method is shown by the proportion-in-area (%). Take the weld metals containing 0.1%P for example, the P solubility is 24 c.p.s. in SUS 304 and 16 s.p.c. in SUS 310S, and consequently the amount of phosphides is less than 0.01% in SUS 304 and about 0.2% in

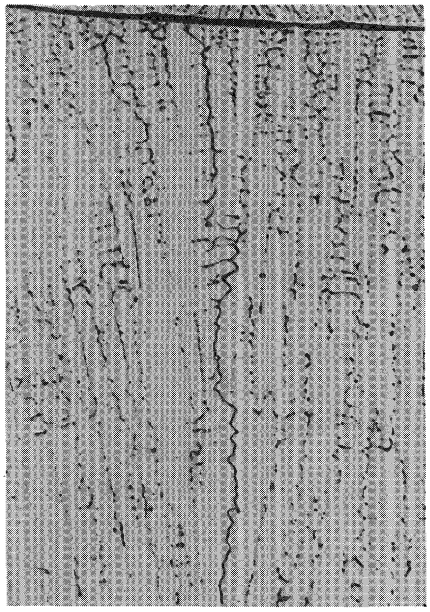

(a)

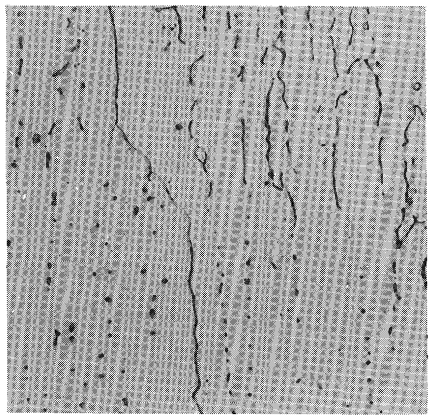

(b)

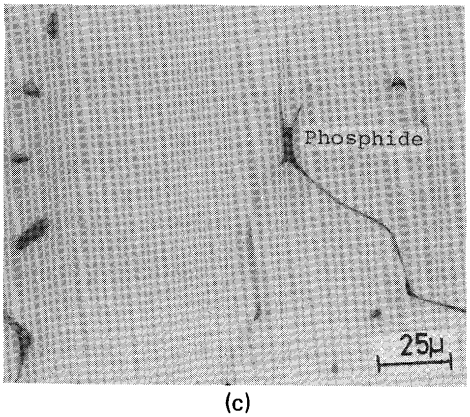

(c)

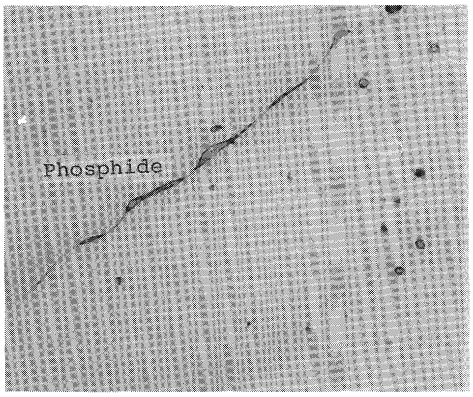

(d)

Photo 12 Microstructures of 310S weld metal, near solidification interface (a) and at about 2.4 mm behind the interface (b) in low magnification, and at about 1250°C (c) and 1100°C (d) in high magnification.

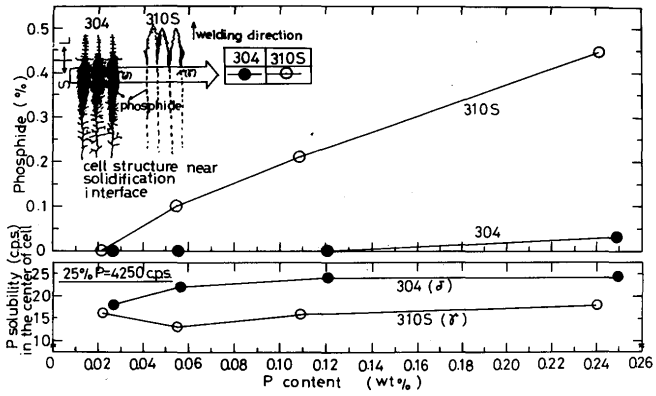

Fig. 15 Comparison of P solubility in cellular dendrite core and consequently phosphide content in weld metals in final stages of solidification between SUS 304 and 310S.

SUS 310S. Except for small amounts of phosphides formed by quenching from liquid lakes enclosed in the solid in case of SUS 304 weld metal containing 0.02 to 0.25%P, phosphides were not found out through the optical microscope. On the other hand, in case of SUS 310S weld metal containing 0.05 to 0.2%P, larger amounts of phosphides formed in the film-like form at the boundary. Moreover, small quantities of phosphides were detected through the SEM even in SUS 310S weld metal containing about 0.02%P. The result in Fig. 14 clearly indicates that there is a little difference in the P solubility in the cellular dendrite core between the primary solidification of δ-ferrite in SUS 304 and the primary solidification of the austenite in SUS 310S and consequently P surely segregated to a higher degree at the boundary in SUS 310S than in SUS 304. This suggests that since the primary solidification of the austenite has a stronger tendency to segregate at the

boundary than the primary solidification of the ferrite, the P element may promote the susceptibility to hot cracking especially in case of the primary solidification of the austenite.

4. Conclusions

The following conclusions are drawn from the fundamental investigations on the solidification structures, the microsegregation during solidification of SUS 304 and 310S weld metals and the effect of S and P on the microsegregation;

(1) Both 304 and 310S weld metals show the features of the cellular dendritic growth mode but make a difference in the solidification process.

(2) In a 304 weld metal the δ-ferrite is primarily formed to a larger extent and subsequently the residual liquid is solidified as the eutectic δ-and γ-phases at the boundary. During subsequent cooling the primary and the eutectic ferrite is drastically transformed to the austenite and a small proportion of the ferrite remains at room temperature, the appearance of which is often observed as if it has been formed at the cellular dendritic boundary. Therefore, we must pay attention to that there is a great difference in the shape and the quantity between the primary and the residual ferrite. The former was formed at a level of about 75 to 80% in area and the content of the latter was about 3.6 to 6% in this investigation. The both contents increased with an increase in the weld heat input.

(3) As regards the equilibrium distribution of alloying elements between δ-and γ-phases at high temperature, austenitizers such as Ni, Mn and C were more soluble in γ-phase and ferritizers such as Cr were more soluble in δ-ferrite.

(4) During solidification, in the 304 weld metal Ni, Mn, Si, S, and P segregated at the cellular dendritic boundaries and in the 310S weld metal Cr, Ni, Mn, Si, S and P segregated. It was particularly noted that in the 310S weld metal P and Si segregated to a higher level.

(5) In 304 and 310S weld metals the increase in the solubility of S in the dendrite core could not be detected by the addition of S deliberately increased. However, in spite of the result that there was no distinct difference in the solubility between the both weld metals, the larger contents of sulphides were formed in 310S than in 304 because S segregates more easily in the primary solidification of the austenite. The addition of S content caused a corresponding increase in the amount of sulphides at the boundary. Sulphides are enriched in S, Mn and Cr in a granular or rod-like form.

(6) The addition of P content showed a little increase in the solubility of P in the cellular dendrite core of the ferrite in 304 weld metal but hardly did in the dendrite core of the austenite in 310S weld metal. The 310S weld metal had a stronger tendency to form phosphides than the 304. The phosphides could be detected even in 310S weld metal containing about 0.02%P, and it almost corresponds to 304 weld metal containing about 0.2%P. In case of 310S weld metal phosphides were predominantly formed in a film-like form along grain boundaries.

Acknowledgements

The authors wish to thank Mr. S. Saruwatari working for Nippon Steel Corporation for his supplying materials and acknowledge the work of Professor I. Okamoto of JWRI for the co-operation of EPMA.

References

1) M. Hasegawa, et al.: Handbook on stainless steels, (1973), (in Japanese)
2) H. Thielsh: "Stainless Steels-Welding Summary", Weld. J., (1955) Jan., pp. 22s–30s.
3) T. G. Gooch and J. Honeycombe: "Microcracking in Fully Austenitic Stainless Steel Weld Metal", Metal Const. & Brit. Weld. J., (1975) Mar., pp. 146–148.
4) H. Thielsch: "Physical Metallugy of Austenitic Stainless Steel", Weld. J., (1950) Dec. pp. 577s–621s.
5) J. Honeycombe and T. G. Gooch: "Effect of Manganese on Cracking and Corrosion Behaviour of Fully Austenitic Stainless-steel Weld-metals", Metal Const. & Brit. Weld. J., (1972) Dec., pp. 456–460.
6) J. Honeycombe and T. G. Gooch: "Effect of Microcracks on Mechanical Properties of Austenitic Stainless-steel Weld-metals", Metal Const. & Brit. Weld. J., (1973) Apr. pp. 140–147.
7) J. C. Borland and R. D. Younger: "Some Aspect of Cracking in Welded Cr-Ni Austenitic Steels", Brit. Weld. J., Vol. 7 (1960), pp 22–59.
8) H. Tamura: "Weld Cracking of Austenitic Stainless Steel", J. Japan Weld. Society, Vol. 41 (1972) No.2, pp.127–147, (in Japanese).
9) F. C. Hull: "Effect of Delta Ferrite on the Hot Cracking of Stainless Steel", Weld. J., (1967), pp. 399s–400s.
10) I. Masumotò, K. Tamaki ans M. Kutsuna: "Hot Cracking of Austenitic Steel Weld Metal", J. Japan Weld. Society, Vol. 41 (1972) No.11, pp.1306–1314. (in Japanese)
11) H. Fredriks and L. J. van der Toorn: "Hot Cracking in Austenitic Stainless Steel Weld Deposits", Brit. Weld. J., 15 (1968) 4, pp.178–182.
12) A. E. Runov: "Reseach on the Hot Cracking Propensities of Fully Austenitic and Duplex Cr-Ni Steels", Svar. Prois., (1971) No.6, pp.24–28.

13) Y. Arata, F. Matsuda and S. Saruwatari: "Varestraint Test for Solidification Crack Susceptibility in Weld Metal of Austenitic Stainless Steels", Trans. JWRI, Vol.3 (1974) No.1, pp.79–88.
14) F. C. Hull: "Effect of Alloying Additions on Hot Cracking of Austenitic Chromium-Nickel Stainless Steels", Pro. Amer. Soc. for Testing and Materials, 60 (1960), pp.667–690.
15) Andre Gueussier and R. Castro: "Etude Experimentale des Criques de Solidification dans les Aciers Influence des Impuretés", Revue de Metallurgie, Vol. 57 (1960) 2, pp.117–134.
16) W. Dahal, C. Druen and H. Musch: "Susceptibility of Austenitic Welded Joints to Hot Cracking", IIW-Doc. II-660-73, IIW-Doc. IX-850-73
17) D. J. Widgery: "Effect of Sulphur and Phosphorus on Weld Metal Solidification Cracking", Metal Const. & Brit. Weld. J., (1970) Aug., pp.333–338.
18) S. M. Makin, C. B. Alcock, D. R. Arkell and P. C. L. Pfeil: "Distribution of Phosphorus and Sulphur in Fully Austenitic Stainless Steel Welds", Brit. Weld. J., (1960) Oct., pp.595–599.
19) H. Fredriksson: "The Solidification Sequence in an 18-8 Stainless Steel, Investigated by Directional Solidification", Metallugical Trans., Vol.3 (1972) Nov., pp.2989–2997.
20) B. Hemsworth, T. Boniszewski and N. F. Eaton: "Classification and Definition of High Temperature Welding Cracks in Alloys", Metal Const. & Brit. Weld. J., (1969) Feb., pp.5–16.
21) G. L. Petrv and V. N. Zemzin: "Influence of Ferrite on Crystallisation Austenitic Weld Metal and the Formation of Hot Cracks during Welding", Svar. Proiz., (1967) No.2, pp.1–3.
22) D. M. Haddrill and R. G. Baker: "Microcracking in Austenitic Weld Metal", Brit. Weld. J., Vo.12 (1965) 8, pp411–419.
23) J. Honeycombe and T. G. Gooch: "Microcracking in Fully Austenitic Stainless Steel Weld Metal", Metal Const. & Brit. Weld. J., (1970) 9, pp.375–380.
24) G. M. Goodwin, N. C. Cole and G. M. Slaughter: "A Study of Ferrite Morphology in Austenitic Stainless Steel Weldments", (1972) Sep., pp.425s–429s.
25) W. T. Delong: "Ferrite in Austenitc Stainless Steel Weld Metal", Weld. J., (1974), pp. 273s–286s.
26) C. H. M. Jenkins, E. H. Bucknall, C. R. Austin and G. A. Mellor: "Some Alloys for Use at High Temperatures", J. Iron & Steel Inst. 136 (1937), pp. 187–222.
27) Y. Otoguro, Y. Kawabe and R. Nakagawa: "Partition of Alloying Elements between Phases and Relation between the Amount of Ferrite and Magnetic Property for Cr-Ni Stainless Steels", Tetsu to Hagane, 59 (1963) No.3, pp.989-996, (in Japanese).